PAPER

Magnetic-Field Dependence of Raman Coupling Strength in Ultracold ^{40}K Atomic Fermi Gas[*]

To cite this article: Liang-Hui Huang *et al* 2016 *Chinese Phys. Lett.* **33** 033401

View the article online for updates and enhancements.

中国物理快报
Chinese Physics Letters

CLICK HERE
for our
Express Letters

Magnetic-Field Dependence of Raman Coupling Strength in Ultracold ^{40}K Atomic Fermi Gas [*]

Liang-Hui Huang(黄良辉)[1,2], Peng-Jun Wang(王鹏军)[1,2], Zeng-Ming Meng(孟增明)[1,2], Peng Peng(彭鹏)[1,2], Liang-Chao Chen(陈良超)[1,2], Dong-Hao Li(李东豪)[1,2], Jing Zhang(张靖)[1,2**]

[1]*State Key Laboratory of Quantum Optics and Quantum Optics Devices, Institute of Opto-electronics, Shanxi University, Taiyuan 030006*
[2]*Collaborative Innovation Center of Extreme Optics, Shanxi University, Taiyuan 030006*

We experimentally demonstrate the relation of Raman coupling strength with the external bias magnetic field in degenerate Fermi gas of ^{40}K atoms. Two Raman lasers couple two Zeeman energy levels, whose energy splitting depends on the external bias magnetic field. The Raman coupling strength is determined by measuring the Rabi oscillation frequency. The characteristics of the Rabi oscillation is to be damped after several periods due to Fermi atoms in different momentum states oscillating with different Rabi frequencies. The experimental results show that the Raman coupling strength will decrease as the external bias magnetic field increases, which is in good agreement with the theoretical prediction.

Ultracold atomic gases are a remarkably rich platform to mimic numerous interesting phenomena in condensed matter and high energy physics,[1] in which the physical parameters can be precisely controlled, including the atomic number, the temperature of ultracold sample, the shape of external trapping potential and the strength of the atom–atom interaction. Recently the scheme of using ultracold atoms to simulate the behavior of electrons in ultracold atom systems has been experimentally realized by using two photon Raman transitions: a pair of Raman laser beams couple resonantly two spin states,[2−10] which opens up an exciting route to study the novel quantum phase, even to yield completely new phenomena with no analogue elsewhere in physics.[11−14] Recently, two-dimensional spin-orbit coupled Fermi gases were realized experimentally by using the Raman-driven tripod energy level configuration, in which three lasers couple with three atomic hyperfine ground states.[15] These breakthroughs lead to a burst of research interest in search for topological insulators, Majorana fermions, dynamical phases, and other novel quantum phases in experiment and theory.[16−20]

The neutral atoms suitably couple with laser fields that can generate an effective gauge field.[21,22] In the Raman coupling method,[23] the Raman coupling strength, one-photon and two-photon detuning of Raman lasers all are the important control parameters in experiment. To achieve the large Raman coupling regime, one should in principle increase the intensity of two Raman beams. Unfortunately there are two difficulties we should face. When we need the strong Raman coupling strength and the less spontaneous emission simultaneously, we try to increase the laser intensity and one-photon detuning of Raman lasers, just like for the optical dipole trap. However, the far one-photon detuning in the Raman process, which is larger than the fine structure splitting of the excited state, cannot further reduce the spontaneous emission loss.[4,14,23,24] In other words, the fine structure splitting of the excited state of alkali atoms determines the ratio of the spontaneous emission loss. The other difficulty is that we need the Raman coupling at the high external magnetic field. The atomic interaction can be tuned by using the magnetic Feshbach resonance. The interesting topological and other exotic superfluids will rise from spin-orbit coupling with s-wave interaction.[13] Therefore, we are interested in how the Raman coupling strength is changed as the homogeneous bias magnetic field is varied. In Ref. [25], the authors calculated the magnetic field dependence for the Raman coupling strength in alkali-metal atoms and found that the Raman coupling strength decreases as the external bias magnetic field increases due to the decoupling mechanism of nuclear and electronic spins in high magnetic field. In this Letter, we experimentally use a pair of Raman lasers to couple two different spin states of degenerate Fermi gas of ^{40}K, and present a detailed study of the dependence of the Raman coupling strength on the external magnetic field from a few Gauss to ∼200 G.

Here we consider the model with two laser beams

**Corresponding author. Email: jzhang74@sxu.edu.cn

coupling two internal hyperfine states of the atom by a stimulated two-photon Raman transition. The stimulated two-photon Raman process means that a photon from one laser beam is absorbed by an atom and stimulated re-emission into another laser beam. Therefore, the momentum of an atom couples to its spin. This scheme has been employed to realize artificial spin-orbit coupling in the Bose–Einstein condensate of ^{87}Rb atoms[3−5] and degenerate Fermi gas.[8,9] We choose the two magnetic sublevels of spin-up $|\uparrow\rangle = |F = 9/2, m_F = -9/2\rangle$ and spin-down $|\downarrow\rangle = |F = 9/2, m_F = -7/2\rangle$ of the $F = 9/2$ hyperfine level of the ^{40}K atomic electronic ground state as the two internal spin states, which are coupled by a pair of Raman beams with coupling strength Ω_R. Two Raman beams oppositely propagate along the $\hat{y}$ direction, which flip atoms from $|\uparrow\rangle$ to $|\downarrow\rangle$ spin states and simultaneously impart momentum $2\hbar k_R$, via the two-photon Raman process. Meanwhile, the two Raman beams are linearly polarized along the $\hat{x}$ and $\hat{z}$ directions, respectively, corresponding to σ and π polarization relative to quantization axis $\hat{z}$ (Fig. 1(a)). The Hamiltonian can be written as

$$\mathfrak{H} = \begin{pmatrix} \frac{\hbar^2}{2m}(p_y - k_R)^2 + \frac{\delta}{2} & \frac{\Omega_R}{2} \\ \frac{\Omega_R}{2} & \frac{\hbar^2}{2m}(p_y + k_R)^2 - \frac{\delta}{2} \end{pmatrix}, (1)$$

where p_y indicates the quasimomentum along the y direction, δ is the two-photon Raman detuning, $\hbar k_R$ is the single-photon recoil momentum of the Raman lasers, and $\hbar$ is Planck's constant. We define the recoil momentum $\hbar k_R = 2\pi\hbar/\lambda$ and the recoil energy $E_R = (\hbar k_R)^2/2m = h \times 8.37$ kHz as the nature momentum and energy units, where m is the atomic mass of ^{40}K, and the wavelength of the Raman beam is $\lambda = 772.4$ nm. The energy gap is $h\Omega_R$ in the momentum space when $h\delta = 4E_R$[4] from Eq. (1).

In our experiment, we first pre-cool the mixture of ^{87}Rb atoms ($\sim 1 \times 10^7$) at the spin state $|F = 2, m_F = 2\rangle$ and ^{40}K atoms ($\sim 4 \times 10^6$) at the spin state $|F = 9/2, m_F = 9/2\rangle$ to 1.5 μK by the rf evaporation cooling in the quadrupole-Ioffe configuration (QUIC) trap, and then transport them into the center of the glass cell in favor of optical access, which is used at previous experiments,[26−28] where F is the quantum number of the atomic total angular momentum, and m_F is the projection along the magnetic direction. Both the species are loaded into the optical dipole trap, and the degenerate Fermi gas of ($\sim 2 \times 10^6$) ^{40}K atoms are obtained in the lowest hyperfine Zeeman state $|F = 9/2, m_F = 9/2\rangle$ by gradually decreasing the depth of the optical trap. The optical dipole trap consists of two far-resonance laser beams, at a wavelength of 1064 nm, crossing in the horizontal plane ($\hat{x} \pm \hat{y}$). The temperature of the Fermi gas is 0.2–0.3T_F, and the Fermi temperature is defined by $T_F = \hbar\bar{\omega}(6N)^{1/3}/k_B$, where $\bar{\omega} = (\omega_x\omega_y\omega_z)^{1/3}$ is the

geometric mean of the optical trap frequency, N is the particle number of ^{40}K atoms, and k_B is Boltzmann's constant. For the ^{40}K degenerate Fermi gas, the optical trap frequency is about $2\pi \times (80, 80, 80)$ Hz along $(\hat{x}, \hat{y}, \hat{z})$. We use a resonant laser beam pulse (780 nm) for 0.03 ms to remove the ^{87}Rb atoms in the mixture without losing and heating ^{40}K atoms. Subsequently, the atoms of the $|F = 9/2, m_F = 9/2\rangle$ state are transferred into the lowest state $|\uparrow\rangle$ in a rapid adiabatic passage induced by sweeping a radio-frequency field across the ten magnetic Zeeman states in $|F = 9/2\rangle$ manifold in 80 ms, where the external magnetic field is about 5 G.
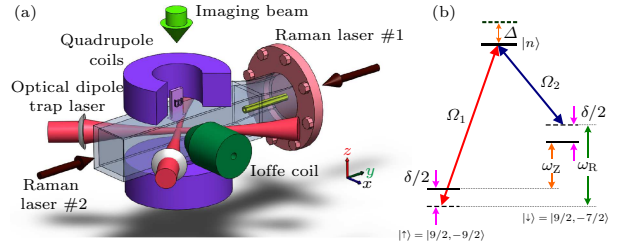

Fig. 1. (Color online) Experimental setup and energy level diagram for the two electronic ground states. (a) Schematic drawing of the experimental setup. The two Raman laser beams are counter-propagating along $\hat{y}$, the external magnetic field B along $\hat{z}$, and the gradient magnetic field is along $\hat{x}$. (b) Level diagram of Raman coupling within the $F = 9/2$ ground state. Here Δ is detuning between the Raman laser field and intermediated excited states $|n\rangle$, δ is the two-photon Raman detuning, Ω_i is the Rabi frequency of laser beam i, ω_R is the Raman frequency difference between two laser beams, and ω_Z is the Zeeman energy difference between both the spin states.

The quadrupole coils with the Helmholtz configuration are used to produce the external bias magnetic field B, which gives a linear Zeeman splitting $\hbar\omega_Z = g\mu_B B$ between two magnetic sublevels along the $\hat{z}$ axis (gravity direction), as shown in Fig. 1(a). A pair of 388.125 THz laser beams are used as the Raman lasers to generate the spin orbit coupling along $\hat{y}$, which are extracted from a continuous-wave Ti-sapphire single frequency laser and focused at the position of the atomic cloud with $1/e^2$ radii of 200 μm, larger than the size of the degenerate Fermi gas. The Raman beams 1 and 2 are frequency-shifted by two acousto-optic modulators (AOM), respectively. Afterwards, the Raman beams are coupled into two polarization maintaining single-mode fibers to increase the stability of the beam pointing and the quality of the beam profile.

To obtain the Raman coupling strength, we measure the periods of Rabi oscillation in ultracold Fermi gas at various external magnetic fields. The degenerate Fermi gases of ^{40}K atoms is first prepared in the optical dipole trap at the $\uparrow$ state. Subsequently, we adiabatically ramp the external magnetic field to a certain value B and hold it for 30 ms to thermal

equilibrium. Afterwards, a pulse of Raman beams is applied to the atoms with a specific power P and frequency difference ω_R to ensure that the two-photon Raman detuning is $\hbar\delta = \hbar(\omega_\mathrm{R} - \omega_\mathrm{z}) = 4E_\mathrm{R}$, where ω_R is the Raman frequency-difference between two laser beams, and ω_z is the Zeeman energy difference between the two spin states. Subsequently, we immediately switch off the optical trap and the magnetic field, and let the atoms ballistically expand in 12 ms and turn on a near resonant light to obtain the time-of-flight (TOF) absorption image. At the final stage, we apply a gradient magnetic field from the Ioffe coil along $\hat{x}$ in the first 10 ms during free expansion, which create a spatial separation of the two spin components corresponding to the Stern–Gerlach effect as shown in Fig. 1(a). Then a number of atoms in each state are independently counted from the TOF image. Lastly we can obtain the curves of the number of atoms in the $|\downarrow\rangle$ state as a function of the duration time of the Raman beam pulse.
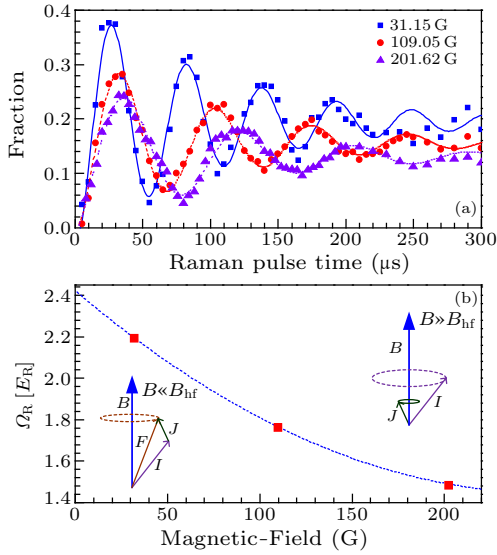

Fig. 2. (Color online) The dependence of Raman coupling strength on the external magnetic field. (a) The population in the ↓ state as a function of the duration time of the Raman beam pulse. Here $B = 31.15$ G for blue squares, $B = 109.05$ G for red circles, and $B = 201.62$ G for purple triangles. The Raman coupling strength $\hbar\Omega_\mathrm{R} = 2.2E_\mathrm{R}$, $1.77E_\mathrm{R}$ and $1.49E_\mathrm{R}$ for the three cases. (b) The Raman coupling strengths of three cases are obtained from Fig. 2(a) as a function of the external magnetic field.

To verify the result that the Raman coupling strength depends on the external magnetic field, we fix the intensity of the Raman lasers and vary the external magnetic field B by changing the current in the quadrupole coils. Afterwards, we obtain the different Rabi oscillating curves for different external magnetic fields as shown in Fig. 2(a). As we all know, the broad s-wave Feshbach resonance of two spin 50/50 states $|\uparrow\rangle$ and $|\downarrow\rangle$ is at $B_0 = 202.1$ G.[29,30] Thus our measurement on the high magnetic field reaches

about 200 G. We observe the phenomena of damped oscillation after several periods.[8] We fit the experimental data with the several periods of oscillation and obtain the curve of Raman coupling strength Ω_R as a function of the external magnetic field B as shown in Fig. 2(b).

The Raman coupling strength Ω_R may be given by[31−33]

$$\Omega_\mathrm{R} = \frac{\Omega_1 \Omega_2}{2\Delta} = -\frac{I_0}{\hbar^2 c\epsilon_0} \sum_n \frac{\langle\downarrow|er_\mathrm{q}|n\rangle\langle n|er_\mathrm{q}|\uparrow\rangle}{\Delta}, \quad (2)$$

where Δ is the one-photon detuning of the Raman lasers, Ω_i is the one-photon Rabi frequency for each of the Raman laser beams i, $I_0 = \sqrt{I_1 I_2}$ is the intensity of the two Raman lasers, $\langle\downarrow|er_\mathrm{q}|n\rangle$ denotes the matrix element that couples the two hyperfine sublevels $|\downarrow\rangle$ and $|n\rangle$ (where the $|\uparrow\rangle$ and $|\downarrow\rangle$ refer to the ground states and the $|n\rangle$ refers to the excited states). As shown in Fig. 1(b), one-photon detuning Δ is changed very little when changing the external magnetic field due to the large one-photon detuning. Thus we can ignore the change of the one-photon detuning Δ when altering the external magnetic field.
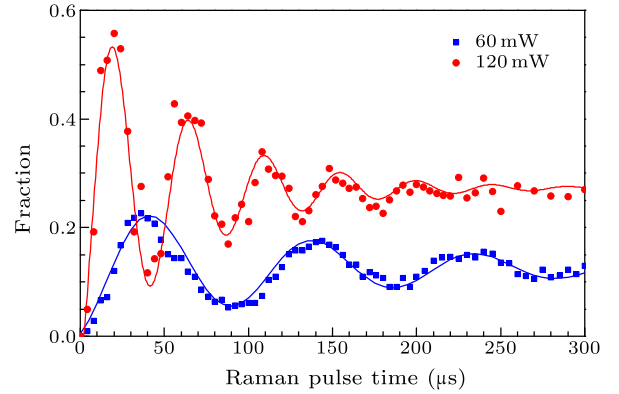

Fig. 3. (Color online) The dependence of Raman coupling strength on the intensity of Raman beams. The population in the ↓ state as a function of the duration time of the Raman beam pulse. The power of Raman beams $P = 60$ mW for blue squares, and $P = 120$ mW for red circles at $B = 206.2$ G. The observed oscillation period $T \approx 92$ and 45 μs correspond to different intensities of the Raman beams.

As in the discussion in Ref. [25] the excited states $|n\rangle$ in Eq. (2) could be expressed as three different cases under the different conditions. One of the cases at the low external magnetic field, the coupling between angular momentum of the nucleus I and the electron J ($I - J$), is strong and the total angular momentum F precesses around the direction of the magnetic field. Then, the spin states are expressed as $|F, m_\mathrm{F}\rangle$. In the higher magnetic field, the $I - J$ coupling is lifted and both angular momenta precess freely around the axis of external magnetic field. Then, the spin state $|n\rangle$ is no longer a pure state in the presence

of a high magnetic field, but a mixture corresponding to $|m_J, m_I\rangle$ as shown the inset in Fig. 2(b). In an extremely strong magnetic field, the electronic spins and the electronic orbital angular momentum are decoupled, and $|n\rangle$ corresponds to $|m_L, m_S, m_I\rangle$. In the intermediate external magnetic field, as in our experiment, the electronic spin and the orbit term become of small perturbation, and the Raman transition matrix element is decreased when the external magnetic field increases, as shown in Fig. 2(b).[34]

Moreover, we show that the frequency of Rabi oscillation for Raman transition is proportional to the intensity of Raman beams in Fig. 3. This is in good agreement with Eq. (2). Thus we can quickly and precisely modify the Raman coupling strength by changing the intensity of Raman lasers in experiment.

In conclusion, we have studied the relationship between the Raman coupling strength and the external magnetic field in ultracold atomic Fermi gases. The Raman coupling strength decreases as the external bias magnetic field increases, which is in good agreement with the theoretical prediction. This work provides a way to explore many unusual behaviors with spin–orbit coupling in a strongly interacting region of ultracold atomic Fermi gases near a Feshbach resonance.

References

[1] Bloch I, Dalibard J and Zwerger W 2008 *Rev. Mod. Phys.* **80** 885
[2] Lin Y J, Compton R L, Jimenez-Garcia K, Porto J V and Spielman I B 2009 *Nature* **462** 628
[3] Lin Y J, Jimenez-Garcia K and Spielman I B 2011 *Nature* **471** 83
[4] Fu Z K, Wang P J, Chai S J, Huang L H and Zhang J 2011 *Phys. Rev. A* **84** 043609
[5] Zhang J Y, Ji S C, Chen Z, Zhang L, Du Z D, Yan B, Pan G S, Zhao B, Deng Y J, Zhai H, Chen S and Pan J W 2012 *Phys. Rev. Lett.* **109** 115301
[6] Qu C L, Hamner C, Gong M, Zhang C W and Engels P 2013 *Phys. Rev. A* **88** 021604(R)
[7] Olson A J, Wang S J, Niffenegger R J, Li C H, Greene C H and Chen Y P 2014 *Phys. Rev. A* **90** 013616
[8] Wang P J, Yu Z Q, Fu Z K, Miao J, Huang L H, Chai S J, Zhai H and Zhang J 2012 *Phys. Rev. Lett.* **109** 095301
[9] Cheuk L W, Sommer A T, Hadzibabic Z, Yefsah T, Bakr W S and Zwierlein M W 2012 *Phys. Rev. Lett.* **109** 095302
[10] Williams R A, Beeler M C, LeBlanc L J, Jiménez-García K and Spielman I B 2013 *Phys. Rev. Lett.* **111** 095301
[11] Galitski V and Spielman I B 2013 *Nature* **494** 49
[12] Goldman N, Juzeliunas G, Ohberg P and Spielman I B 2014 *Rep. Prog. Phys.* **77** 126401
[13] Zhang J, Hu H, Liu X J and Pu H 2014 *Annu. Rev. Cold At. Mol.* **2** 81
[14] Zhai H 2015 *Rep. Prog. Phys.* **78** 026001
[15] Huang L H, Meng Z M, Wang P J, Peng P, Zhang S L, Chen L C, Li D H, Zhou Q and Zhang J 2015 arXiv:1506.02861 [cond-mat.quant-gas]
[16] Dong Y, Dong L, Gong M and Pu H 2015 *Nat. Commun.* **6** 6103
[17] Campbell D L, Juzeliunas G and Spielman I B 2011 *Phys. Rev. A* **84** 025602
[18] Qin F, Wu F, Zhang W, Yi W and Guo G C 2015 *Phys. Rev. A* **92** 023604
[19] Mulkerin B C, Fenech K, Dyke P, Vale C J, Liu X J and Hu H 2015 arXiv:1509.08225[cond-mat.quant-gas]
[20] Sun K, Qu C L, Xu Y, Zhang Y P and Zhang C W 2015 arXiv:1510.03787[cond-mat.quant-gas]
[21] Juzeliunas G and Ohberg P 2008 *Structured Light and its Applications: Optical Manipulation of Ultracold Atoms* (Amsterdam: Elevier)
[22] Dalibard J, Gerbier F, Juzeliunas G and Ohberg P 2011 *Rev. Mod. Phys.* **83** 1523
[23] Spielman I B 2009 *Phys. Rev. A* **79** 063613
[24] Mueller E J 2012 *Physics* **5** 96
[25] Wei R and Mueller E J 2013 *Phys. Rev. A* **87** 042514
[26] Wei D, Chen H X and Zhang J 2007 *Chin. Phys. Lett.* **24** 679
[27] Wei D, Xiong D Z, Chen H X, Wang P J, Guo L and Zhang J 2007 *Chin. Phys. Lett.* **24** 1541
[28] Xiong D Z, Chen H X, Wang P J, Yu X D, Gao F and Zhang J 2008 *Chin. Phys. Lett.* **25** 843
[29] Gaebler J P, Stewart J T, Drake T E, Jin D S, Perali A, Pieri P and Strinati G C 2010 *Nat. Phys.* **6** 569
[30] Genkina D, Aycock L M, Stuhl B K, Lu H I, Williams R A and Spielman I B 2015 arXiv:1501.00036 [physics.optics]
[31] Jaksch D and Zoller P 2003 *New J. Phys.* **5** 56
[32] Miyake H 2013 PhD Dissertation (America: Massachusetts Institute of Technology)
[33] Huang L H, Wang P J, Fu Z K and Zhang J 2014 *Acta Opt. Sin.* **34** 0727002 (in Chinese)
[34] Ludewig A 2012 PhD Dissertation (Holland: Universiteit van Amsterdam)